ResearchGate

See discussions, stats, and author profiles for this publication at: https://www.researchgate.net/publication/365614558

In vitro antiplasmodial, molecular docking and pharmacokinetics studies of specialized metabolites from Tetrapleura tetraptera (Fabaceae)

Article *in* South African Journal of Botany · November 2022

DOI: 10.1016/j.sajb.2022.11.021

CITATIONS
3

READS
37

7 authors, including:



Klev Gaïtan Sikam
University of Douala
8 PUBLICATIONS **17** CITATIONS
SEE PROFILE



Gervais Mouthé Happi
THE UNIVERSITY OF BAMENDA
47 PUBLICATIONS **347** CITATIONS
SEE PROFILE



Sikiru Akinyeye Ahmed
Kwara State University
24 PUBLICATIONS **103** CITATIONS
SEE PROFILE



Wakeu Kweka Brussine Nadege
University of Yaounde I
6 PUBLICATIONS **41** CITATIONS
SEE PROFILE

Some of the authors of this publication are also working on these related projects:

Yaoundé-Bielefeld Graduate School for Natural Products with Antiparasite and Antibacterial Activity View project

NAPEC laboratory View project

All content following this page was uploaded by Gervais Mouthé Happi on 21 November 2022.

The user has requested enhancement of the downloaded file.

South African Journal of Botany 151 (2022) 949–959

Contents lists available at ScienceDirect

South African Journal of Botany

journal homepage: www.elsevier.com/locate/sajb

In vitro antiplasmodial, molecular docking and pharmacokinetics studies of specialized metabolites from *Tetrapleura tetraptera* (Fabaceae)

Klev Gaïtan Sikam[a], Gervais Mouthé Happi[b,*], Sikiru Akinyeye Ahmed[c], Brussine Nadege Kweka Wakeu[d], Livine Zemo Meikeu[b], Shina Salau[c], Jean Duplex Wansi[a,*]

[a] Department of Chemistry, Faculty of Sciences, University of Douala, P.O. Box 24157 Douala, Cameroon
[b] Department of Chemistry, Higher Teacher Training College, The University of Bamenda, P.O Box 39 Bambili, Cameroon
[c] Department of Chemistry and Industrial Chemistry, Kwara State University, Malete, P.M.B 1530 Ilorin, 23431, Nigeria
[d] Department of Organic Chemistry, Faculty of Sciences, University of Yaounde I, P.O. Box 812 Yaounde, Cameroon

ARTICLE INFO

Article History:
Received 18 September 2022
Revised 12 November 2022
Accepted 14 November 2022
Available online xxx

Edited by: Dr S.C. Pendota

Keywords:
ADMET study
Fabaceae
Molecular docking
Plasmodium falciparum
Tetrapleura tetraptera

ABSTRACT

Tetrapleura tetraptera is a well-known plant widely used in Cameroon as spices in cooking and in preparations prescribed in folk medicine for the treatment of malaria. The main purpose of this study was to provide relevant chemical and pharmacological insights that can support the effectiveness of *T. tetraptera* against malaria by identifying the lead compounds that may be responsible for its therapeutic potential. The stem bark and root methanolic crude extracts of this plant displayed a good inhibition of *P. falciparum* 3D7 with rates of 83.6% and 76.3%, respectively. A total of sixteen distinct compounds (**1**–**16**) have been isolated during the chemical investigations of the two active crude extracts. Their structures were established with the aid of their NMR data. Thriteen compounds (**2**–**9, 11**–**13, 15** and **16**) were screened for antiplasmodial activity using *P. falciparum* 3D7. Results showed that seven tested compounds displayed good activity ($IC_{50} < 7\ \mu M$) and the most effective were compounds **5, 9, 7, 2** and **6** with IC_{50} values of ($1.8 \pm 0.4\ \mu M$), ($1.9 \pm 0.8\ \mu M$), ($2.1 \pm 0.5\ \mu M$), ($2.3 \pm 0.7\ \mu M$), ($2.4 \pm 0.6\ \mu M$), respectively. The *in silico* evaluation of the isolated compounds for their ability to inhibit the *P. falciparum* dihydroorotate dehydrogenase 5TBO and their ADMET studies revealed that up to fifteen isolated compounds displayed a greater affinity to the binding site of the 5TBO receptor compared to the reference drug chloroquine. More especially, compounds **1, 2, 4, 8** and **14** demonstrated a good drug-likeness. These findings support the use of *T. tetraptera* for the management of malaria and further qualify it as an important source of good candidates in new antiplasmodial drug development.

© 2022 SAAB. Published by Elsevier B.V. All rights reserved.

1. Introduction

Spices are not only food additives that improve the taste and smell of food, they also represent historical seals of different cultures that have an important impact on human health (Bukvicki et al., 2020). Indeed, *Zingiber officinal* is used for the treatment of inflammation and cancer (Ghosh et al., 2011) while *Xylopia aethioica* is a good antiplasmodial agent (Larayetan et al., 2022). Malaria is a life-threatening disease caused by *Plasmodium* parasites, which are transmitted to humans by infected female *Anopheles* mosquito bites (Happi et al., 2015). According to a recent report by World Health organisation (WHO) on malaria in 2021, there were around 241 million cases of malaria worldwide and the African region carries a high share of the global malaria burden including 96% of malaria death among which 80% were children under 5 (Bongmo et al., 2022). More especially, the prescribed drugs to cure malaria like chloroquine, artemisinin or quinine faced some resistance against *Plasmodium falciparum*, which is responsible for the most severe forms of malaria and the high rate of death (Happi et al., 2022; Mutabingwa et al., 2005; Williams et al., 2004). It is therefore urgent to intensify the prospection of new sources of molecules endowed with anti-malarial activity as well as the search for molecules and/or association of molecules that can potentiate the action of chloroquine and artemisinin, which are today the first-line and most accessible drugs in developing countries. In this regard, Cameroonian medicinal plants represent a good source of molecules with several biological activities (Mbobda et al., 2021; Keugwa et al., 2021; Happi et al., 2020; Tabekoueng et al., 2020; Kemayou et al., 2020).

Tetrapleura tetraptera belonging to the family Fabaceae is a tree that grows in the tropical deciduous forest of West Africa, extending from Senegal to West Cameroon (Burkill et al., 1995). It is a single-stemmed, robust, perennial tree of 15–20 m in height, with dark

* Corresponding authors.
E-mail addresses: gervais20022003@yahoo.fr (G.M. Happi), jdwansi@yahoo.fr (J.D. Wansi).

https://doi.org/10.1016/j.sajb.2022.11.021
0254-6299/© 2022 SAAB. Published by Elsevier B.V. All rights reserved.

green leaves and a thick, woody base and spreading branches. Its leaves are 25 to 30 cm long, while the leaflets flattened at their ends, are 3 to 4 cm. The fruits are 10 to 30 cm long and possess a flagrant, which has been attributed to their insect repellent property (Ojewole et al., 2004). *T. tetraptera* is a popular spice in Africa and is locally known as "Essesse" in Douala (Cameroon) or "Aidan" in Nigeria (Adewunmi et al., 1993). The fruits of *Tetrapleura tetraptera* are used for therapeutic soups preparations for nannies to prevent contractions postpartum (Adesina et al., 2016). When dried, they are also used in traditional medicine to fight against several diseases including malaria (Kemigisha et al., 2018; Irvine et al., 1961; Dalziel et al., 1955). As part of our program of the search for antiplasmodial compounds from local medicinal plants, we have chemically and biologically investigated the bark and roots of *T. tetraptera* harvested in the West region of Cameroon to obtain significant findings that can further strengthen the use of the plant by local population against malaria. Furthermore, the molecular docking of all the isolated compounds and their ADMET study are herein discussed.

2. Materials and methods

2.1. General instrumentation

EI-MS and ESI-MS were recorded on a Finnigan MAT 95 spectrometer (70 eV) with perfluorokerosene as a reference substance for EI−HR−MS. The spectrometer operated in positive and negative modes (*m/z*: 50−1500, with a scan rate of 1.00 Hz) with automatic gain control to provide high-accuracy mass measurements within 1 ppm deviation using Na formate as calibrant. The following parameters were used for experiments: spray voltage of 4.5 kV, the capillary temperature of 200 °C. Nitrogen was used as sheath gas (4 l/min). The ^{1}H- and ^{13}C NMR spectra were recorded at 500 MHz and 125 MHz, respectively on Bruker AMX 500 NMR spectrometers chemical shifts are reported in δ (ppm) using TMS as internal standard and coupling constants (J) were measured in Hz. Column chromatography was carried out on silica gel (70–230 mesh, Merck). Thin-layer chromatography (TLC) was performed on Merck precoated silica gel 60 F_{254} aluminum foil, and spots were detected using ceric sulfate spray reagent.

2.2. Plant material

The stem bark and root of *Tetrapleura tetraptera* (Schum. & Thonn.) Taub. were collected at Bafang (GPS coordinates: Latitude 5° 09′32″N, Longitude 10°11′28″E, Elevation: 1280 m) in the West region of Cameroon in September 2020. The identification of the plant was made by the botanist Mr. Victor Nana at the National Herbarium of Cameroon, where a specimen was kept under the voucher number 31,310 HNC.

2.3. Extraction and isolation

The air-dried and powdered bark (2.6 kg) and roots (4.2 kg) of *Tetrapleura tetraptera* were separately macerated twice at room temperature with methanol for 48 h and 24 h, successively. After filtration, the filtrates were evaporated under reduced pressure, to obtain 82.6 g and 182.8 g of crude extract from bark and roots, respectively. Approximately 5 g of each extract were kept for biological assays.

The remaining stem bark crude extract (77.6 g) was chromatographed over silica gel (70−230 mesh) by increasing polarity using a gradient of ethyl acetate (AcOEt) in n-hexane (*n*-Hex), follows by the gradient of methanol (MeOH) in EtOAc. A total of 487 sub-fractions (200 ml each) were collected and combined on the basis of their TLC profiles resulting in seven main fractions A–G. In the following, fraction A (11.5 g, combined sub-fractions 1–85) was rechromatographed over silica gel column (230−400 mesh, 3.5 × 50.0 cm) with *n*-Hex/EtOAc (19:1) yielding a white powder identified as lupeol (**3**) (15.3 mg). Fraction B (22.4 g, combined sub-fractions 86–122) was also rechromatographed over silica gel column (230−400 mesh, 3.5 × 50.0 cm) with *n*-Hex/EtOAc (9:1). Sub-fractions 100–122 yielded white powder identified as betulinic acid (**6**) (12.1 mg). By applying the same method, the third main fraction C (15.0 g, combined sub-fractions 123–155) with *n*-Hex/EtOAc (17:3) gave a white amorphous powder identified as betulin (**5**) (4.7 mg). Fraction D (10.7 g, combined sub-fractions 156–225) was further purified using the same technique eluting the column with *n*-Hex/EtOAc (4:1). Sub-fractions 209–225 gave ursolic acid (**11**) (14.7 mg). Fraction E (11.2 g, combined sub-fractions 226–335) was purified using column chromatography with a gradient of EtOAc (10–20%) in *n*-Hex to afford butein (**2**) (8.5 mg).

The remaining roots crude extract (177.8 g) was partitioned using flash chromatography with EtOAc, EtOAc/MeOH 3:1 and MeOH. Filtrates were separately evaporated under reduced pressure, to obtain three main fractions R1–R3, respectively. Fraction R1 (68.3 g) was dissolved in methanol, adsorbed onto silica gel (70−230 mesh) and subjected to gravity CC on a column packed with silica gel (200 g, 5 cm diameter x 80 cm length). A solvent gradient starting with *n*-Hex and gradually increasing the polarity using EtOAc and MeOH, and fractions of 200 ml were collected. On the basis of TLC analysis, the fractions obtained were combined and yielded 8 sub-fractions (A–H). sub-fraction A (*n*-Hex/EtOAc 39:1) was subjected to further purification using column chromatography and yielded stigmasterol (**15**) (8.2 mg) and 3β-taraxeryl acetate (**13**) (7.8 mg). After similar processing to other sub-fractions, sub-fraction B (*n*-Hex/EtOAc 19:1) yielded lupenone (**4**) (4.1 mg), sub-Fraction E (*n*-Hex/EtOAc 11:9) yielded rhusopolyphenol (**1**) (3.4 mg) while sub-fraction F (*n*-Hex/EtOAc 1:1) gave maslinic acid (**7**) (14.9 mg). Elution of fraction R2 on column chromatography using a mixture of *n*-Hex/EtOAc (2:3), EtOAc and methanol of increasing polarities, afforded 6 sub-fractions (I–N) on the basis of TLC analysis. Purification of sub-fraction I (*n*-Hex/EtOAc 2:3) yielded tormentic acid (**12**) (10.3 mg) and stigmasterol-3-*O*-β-D-glucopyranoside (**16**) (9.2 mg). After similar processing with the other sub-fractions, we obtained from sub-fraction L eluted with EtOAc arjungenin (**8**) (3.2 mg). Sub-fraction M (EtOAc/MeOH 19:1) afforded rhaponticin (**14**) (4.3 mg), aridanin (**9**) (21.3 mg) and hederagenin-3-*O*-α-L-arabinopyranoside (**10**) (3.8 mg).

2.4. Antiplasmodial activity

2.4.1. Parasitic culture

Plasmodium falciparum 3D7 strain (chloroquine-sensitive) was obtained from the Biodefense and Emerging Infections (BEI) Research Resources (Manassas, VA) and maintained in vitro using a modified method previously described by Trager and Jensen (1976). Briefly, parasites were cultured in fresh O^{+} human red blood cells at 3% (v/v) hematocrit in RPMI 1640 culture media containing glutamax and $NaHCO_3$ (Gibco, UK), supplemented with 25 mM HEPES (Gibco, UK), 1X hypoxanthine (Gibco, USA), 20 μg/mL gentamicin (Gibco, China), and 0.5% Albumax II (Gibco, USA). When needed, parasites were synchronized at the ring stage by sorbitol treatment and cultured through one cycle before treatment. Parasite cultures of *P. falciparum* were synchronized by 5% D-sorbitol treatment to obtain only ring-stage parasitized cells. 1% ring stage of parasitemia was maintained for antimalarial assay.

2.4.2. In vitro antiplasmodial assay

The crude methanolic extracts and the isolated compounds were screened in vitro by the modified schizont maturation inhibition assay method described by Sahoo et al. (2020). Stock solutions (10 mM) were prepared by dissolving the crude extracts and pure compounds into DMSO and subsequent dilutions were made in triplicate with an incomplete RPMI medium containing the tested samples

at different concentrations with parasite cultures (1% parasitemia and 1.5% hematocrit) in 96-well plates to a final drug concentration of 10 μM for hit identification studies, or 10 – 0.078 μM for activity confirmation assays. The final dimethyl sulfoxide (DMSO) concentration per 100 μL culture per well was 0.1%. Chloroquine at a range of 1 – 0.0078 μM each was used as negative growth control (positive test control), while the solvent-treated culture (0.1% DMSO) was used as positive growth control (negative test control). Following 72 h incubation at 37 °C and 5% CO_2 humidified atmosphere. Thin smears of the slide were prepared after the incubation period from each well. 3% Giemsa stain was used to stain each slide and examined under a microscope. The level of parasitemia in terms of schizont inhibition was calculated by counting the number of schizonts against 200 asexual parasites microscopically. The schizonts inhibition (%) of each concentration of various fractions and isolated compounds was calculated by following formulae. Schizonts inhibition (%) = no. of schizonts (control) – no. of schizonts (test)/no. of schizonts (control) x 100. IC_{50} values (inhibitory concentrations that reduce 50% parasitic growth compared to control) were calculated and expressed as mean ± SD (n = 3).

2.4.3. Statistical analysis

All the experiments were done in triplicate and the data obtained from the analyses were expressed as mean ± SD (n = 3). The data were statistically analysed using one-way ANOVA and SigmaPlot 12.5 software. The level of significance in all statistical tests was $p < 0.05$.

2.5. Computational methodology

2.5.1. Computational tools

To all the *In silico* studies applied into this work were achieved using the following computational tool:

a ACDChemSketch® version 2020.2.0 used for modeling, first-hand, chemical structures to be fed for docking screening (ACD/ChemSketch, 2020)
b Autodock Vina® tool used for the virtual screening procedure (Trott and Olson, 2010)
c BIOVIA® Discovery Studio version 2021 used for determination of binding pockets and for visualizing/analyzing the docked results (Biovia, 2021)
d Absorption Distribution Metabolism Excretion and Toxicity of Structure Activity-Relationship (ADMETSAR): A web server used to evaluate the ADMET properties, biological activity and drug likeness (Yang et al., 2018; Daina et al., 2017; Cheng et al., 2012; Tsaioun and Kates, 2010)

2.5.2. Molecular docking

The virtual screening was done on *Tetrapleura tetraptera* containing sixteen compounds using the Autodock vina® (Trott and Olson, 2010) tool and Biovia Discovery Studio (Biovia, 2021). The screening was guided using chloroquine a well-known antiplasmodial drug, as standards.

2.5.2.1. Ligand preparations. In a quest to predict the anti-plasmodial activity of the plant samples, compounds isolated from *T. tetraptera* were modeled using the ACDChem ChemSketch® (ACD/ChemSketch, 2020) computational tool and fed into Autodock vina® (Trott and Olson, 2010) for binding efficiency screening.

2.5.2.2. Receptor preparations. The Anti-plasmodium receptor of PDB CODE: 5TBO, was used as target receptor for this study. The receptor was obtained from the (RCSB) database (http//www.rcsb.org/pdb). The resolution of receptor 5TBO (2.15 Å) approximately lies about the 2.0 Å recommended resolution for a receptor of good quality (Falade et al., 2021). Water molecules around the crystal structure and other associated inhibitors were removed from the downloaded protease to avoid undesired interferences and unwanted molecular interactions.

2.5.2.3. Virtual screening. The docking simulation (virtual screening) was done via the Pyrx/Vina tool (Trott and Olson, 2010) Auto Dock Tools (ADT) was used to generate the autodock file (*.pdbqt* file) in preparation for docking. Other adjustments performed on both crystal structures includes, removing any extra water molecules, adding polar hydrogens, merging no-polar hydrogens, and adding Kollman charges. These adjustments are targeted at improving the affinity of the binding site. In modern Computer Assisted Drug Design (CADD), the study of a potent drug is not complete without the activity study of the drug which is deducible from the compound's inhibition constant. A potent compound is expected to have inhibition constant values ranging between 0.01 and 1 μM for a potent drug, therefore, this parameter alone is enough to screen compounds in the drug discovery journey (Falade et al., 2021).

2.5.3. ADMET studies

Absorption (Human Intestinal Absorption), Distribution (Blood Brain Barrier; Water solubility), Metabolism (Cytochrome inhibition: CYP450), Excretion (Half-life) and Toxicity (hERG inhibition; Carcinogenicity) were predicted using the ADMETlab 2.0 web server online (Xiong et al., 2021). From the server, the drug-Brain-Blood-Barrier crossing, drug induced hERG toxicity, drug metabolism, water solubility and drug likeness were computed.

3. Results and discussion

3.1. Phytochemical study

The chemical investigation carried out on the bark and roots of *Tetrapleura tetraptera* led to the isolation and identification of sixteen specialized compounds (Fig. 1). The structures of all the compounds have been determined using their recorded spectrometric and spectroscopic data which were further compared with those reported in the literature to further support their elucidation. Thus, the sixteen compounds have been sorted into two chalcones identified as rhusopolyphenol F (**1**) (Kim et al., 2013) and butein (**2**) (Song et al., 2013); four lupane-type triterpenoids namely lupeol (**3**) (Bongmo et al., 2022; Miranda et al., 2015), lupenone (**4**) (Kweka et al., 2022), betulin (**5**) (Ahmadu et al., 2021) and betulinic acid (**6**) (Happi et al., 2021; Wahab et al., 2021); four oleanane-type triterpenoids viz maslinic acid (**7**) (Miranda et al., 2015), arjungenin (**8**) (Honda et al., 1976), aridanin (**9**) (Adesina et al., 1985) and hederagenin-3-*O*-α-L-arabinopyranoside (**10**) (Jhoo et al., 2021); two ursane-type triterpenoids identified as ursolic acid (**11**) (Seebacher et al., 2003) and its congener tormentic acid (**12**) (An et al., 2011). Furthermore, 3β-taraxeryl acetate (**13**) (Abouelela et al., 2018) has been obtained as the unique taraxane-type triterpenoids along with one stilbenoid glucoside rhaponticin (**14**) (Bongmo et al., 2022) as well as two common steroids stigmasterol (**15**) and stigmasterol-3-*O*-β-D-glucopyranoside (**16**) (Tsopgni et al., 2019).

The yields of the fourteen isolated compounds from the stem bark and root of *T. tetraptera* are listed in Table 1. Aridanin (**9**) was the major compound from the root extract with a yield of 0.012%, while betulin (**5**) was the most abundant compound in the stem bark extract with a yield of 0.06%. The result was in agreement with the literature reporting *Tetrapleura tetraptera* as an important source of aridanin (Sikam et al., 2022)

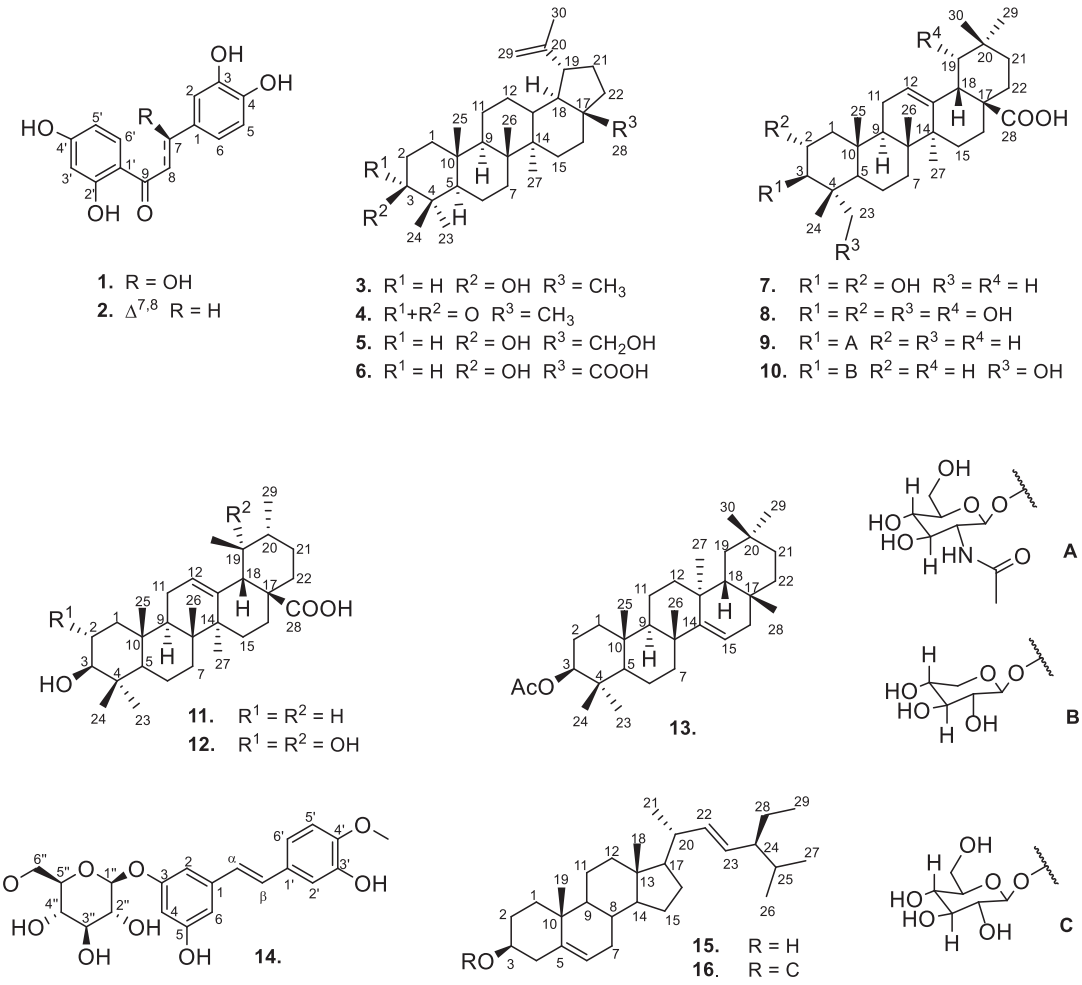


Fig. 1. Chemical structures of compounds isolated from *Tetrapleura tetraptera*.

3.2. Aspects and spectroscopic data of isolated compounds

Rhusopolyphenol F (**1**) – Orange-yellow powder. ^{1}H NMR (CD_3OD, 500 MHz) δ: 7.74 (1H, d, J = 8.7 Hz, H-6′), 6.95 (1H, d, J = 8.2 Hz, H-5), 6.81 (1H, d, J = 2.3 Hz, H-2), 6.79 (1H, dd, J = 2.3, 8.2 Hz, H-6), 6.51 (1H, dd, J = 2.3, 8.7 Hz, H-5′), 6.37 (1H, d, J = 2.3 Hz, H-3′), 5.33 (1H, dd, J = 2.9, 12.9 Hz, H-7), 3.07 (1H, dd, J = 12.9, 16.9 Hz, H-8b), 2.71 (1H, dd, J = 3.0, 16.9 Hz, H-8a); ^{13}C NMR (CD_3OD, 125 MHz) δ: 192.5 (C-9), 165.4 (C-4′), 164.2 (C-2′), 145.4 (C-4), 145.1 (C-3), 130.6 (C-6′), 128.4 (C-1), 117.8 (C-5′), 114.8 (C-5), 113.6 (C-2), 113.2 (C-1′), 110.3 (C-6), 102.4 (C-3′), 79.6 (C-7), 43.6 (C-8).

Butein (**2**) – Orange-yellow powder. ^{1}H NMR (CD_3OD, 500 MHz) δ: 7.96 (1H, d, J = 8.7 Hz, H-6′), 7.72 (1H, d, J = 15.3 Hz, H-β), 7.56 (1H, d, J = 15.3 Hz, H-α), 7.20 (1H, d, J = 2.1 Hz, H-2), 7.13 (1H, dd, J = 2.1, 8.2 Hz, H-6), 6.84 (1H, d, J = 8.2 Hz, H-5), 6.44 (1H, dd, J = 2.4, 8.7 Hz, H-5′), 6.31 (1H, d, J = 2.4 Hz, H-3′); ^{13}C NMR (CD_3OD, 125 MHz) δ: 192.8 (C-9), 166.1 (C-2′), 164.9 (C-4′), 148.5 (C-4), 147.7 (C-7), 145.4 (C-3), 131.8 (C-6′), 127.0 (C-1), 122.2 (C-6), 116.8 (C-8), 115.2 (C-5), 114.4 (C-2), 113.3 (C-1′), 107.7 (C-5′), 102.4 (C-3′).

Lupeol (**3**) – White powder. ^{1}H NMR ($CDCl_3$, 600 MHz) δ: 4.71 (1H, d, J = 4.0 Hz, H-29b), 4.69 (1H, d, J = 4.0 Hz, H-29a), 3.21 (1H, dd, J = 11.5, 4.7 Hz, H-3), 2.41 (1H, *m*, H-19), 1.93 (1H, m, H-21b), 1.70 (3H, s, H-30), 1.69 (1H, m, H-15b), 1.67 (3H, m, H-1b, H-12b, H-13), 1.62 (1H, m, H-2a), 1.59 (1H, m, H-2b), 1.52 (1H, m, H-6a), 1.47 (1H, m, H-16b), 1.43 (1H, m, H-11a), 1.42 (1H, m, H-6b), 1.41 (2H, m, H-7), 1.40 (1H, m, H-22b), 1.39 (1H, m, H-18), 1.38 (1H, m, H-16a), 1.33 (1H, m, H-21a), 1.28 (1H, m, H-9), 1.23 (1H, m, H-11b), 1.21 (1H, m, H-22a), 1.07 (3H, s, H-26), 1.05 (1H, m, H-12a), 0.99 (1H, m, H-15a), 0.97 (3H, s, H-27), 0.95 (3H, s, H-28), 0.92 (1H, m, H-1a), 0.86 (3H, s, H-25), 0.81 (3H, s, H-24), 0.78 (3H, s, H-23), 0.72 (1H, m, H-5); ^{13}C NMR ($CDCl_3$, 150 MHz) δ: 148.2 (C-20), 109.5 (C-29), 79.0 (C-3), 55.1 (C-5), 53.9 (C-18), 50.1 (C-9), 48.7 (C-17), 47.9 (C-19), 44.2 (C-22), 42.3 (C-14), 41.7 (C-8), 40.2 (C-16), 38.9 (C-1), 38.7 (C-4), 37.1 (C-10), 33.4 (C-7), 32.7 (C-13), 28.0 (C-23), 27.4 (C-2, C-21, C-15), 23.9 (C-12), 20.9 (C-11), 19.6 (C-30), 18.4 (C-6), 16.9 (C-28), 16.6 (C-25), 15.9 (C-26), 15.4 (C-24), 15.1 (C-27).

Table 1
Yield (w/w) of isolated compounds from T. tetraptera extracts.

Compounds	Stem bark	Root
1	/	0.002%
2	0.011%	/
3	0.02%	/
4	/	0.002%
5	0.06%	/
6	0.016%	/
7	/	0.008%
8	/	0.002%
9	/	0.012%
10	/	0.002%
11	0.019%	/
12	/	0.006%
13	/	0.004%
14	/	0.002%
15	/	0.005%
16	/	0.005%

Lupenone (**4**) – White powder. ^{1}H NMR ($CDCl_3$, 600 MHz) δ: 4.72 (1H, d, *J* = 4.0 Hz, H-29a), 4.70 (1H, d, *J* = 4.0 Hz, H-29b), 2.53 (1H, m, H-2a), 2.42 (1H, m, H-2b), 1.96 (1H, m, H-1b), 1.72 (1H, m, H-1a), 1.70 (3H, s, H-30), 1.10 (3H, s, H-23), 1.06 (3H, s, H-24), 1.04 (3H, s, H-27), 0.97 (3H, s, H-26), 0.96 (3H, s, H-25), 0.71 (3H, s, H-28); ^{13}C NMR ($CDCl_3$, 150 MHz) δ: 218.2 (C-3), 148.2 (C-20), 109.5 (C-29), 54.9 (C-5), 53.8 (C-18), 49.7 (C-9), 48.8 (C-17), 47.9 (C-19), 47.7 (C-4), 44.2 (C-22), 42.3 (C-14), 41.7 (C-8), 40.2 (C-16), 39.6 (C-1), 36.9 (C-10), 34.2 (C-2), 32.7 (C-7), 32.7 (C-13), 27.4 (C-21), 26.6 (C-23), 23.9 (C-15), 21.6 (C-12), 21.1 (C-11), 20.9 (C-24), 19.8 (C-30), 19.7 (C-6), 16.6 (C-27), 16.5 (C-26), 15.8 (C-25), 15.2 (C-28).

Betulin (**5**) - White amorphous powder. ^{1}H NMR ($CDCl_3$, 500 MHz) δ: 4.67 (1H, d, *J* = 4.0 Hz, H-29b), 4.51 (1H, d, *J* = 4.0 Hz, H-29a), 3.79 (1H, d, *J* = 10.8 Hz, H-28b), 3.31 (1H, d, *J* = 10.8 Hz, H-28a), 3.16 (1H, dd, *J* = 10.5, 5.0 Hz, H-3), 1.69 (3H, s, H-30), 1.64 (1H, m, H-2a), 1.62 (1H, m, H-1b), 1.60 (1H, m, H-2b), 1.01 (3H, s, H-27), 0.99 (3H, s, H-26), 0.96 (3H, s, H-23), 0.91 (1H, m, H-1a), 0.82 (3H, s, H-25), 0.76 (3H, s, H-24), 0.66 (1H, m, H-5); ^{13}C NMR ($CDCl_3$, 125 MHz) δ: 150.5 (C-20), 109.8 (C-29), 79.0 (C-3), 60.5 (C-28), 53.3 (C-5), 50.5 (C-9), 48.8 (C-19), 47.9 (C-18), 47.7 (C-17), 42.6 (C-14), 41.1 (C-8), 39.7 (C-1), 38.8 (C-4), 37.3 (C-13), 37.1 (C-10), 34.4 (C-7), 34.0 (C-22), 29.7 (C-21), 29.3 (C-16), 28.0 (C-23), 27.6 (C-2), 27.4 (C-15), 25.3 (C-12), 20.9 (C-11), 19.6 (C-30), 18.4 (C-6), 16.1 (C-27), 16.1 (C-25), 16.1 (C-24), 16.0 (C-26).

Betulinic acid (**6**) - White powder. ^{1}H NMR ($CDCl_3$, 500 MHz) δ: 4.71 (1H, m, H-29a), 4.58 (1H, m, H-29b), 3.31 (1H, ddd, *J* = 5.0, 16.9, 10.5 Hz, H-19), 3.21 (1H, dd, *J* = 11.5, 4.7 Hz, H-3), 2.35 (1H, m, H-13), 2.24 (1H, m, H-16b), 1.94 (1H, m, H-15b), 1.69 (3H, s, H-30), 1.67 (1H, m, H-1b), 1.64 (1H, m, H-12b), 1.61 (1H, m, H-18), 1.58 (2H, m, H-2), 1.52 (1H, m, H-6a), 1.42 (1H, m, H-6b), 1.41 (1H, m, H-11a), 1.40 (1H, m, H-16a), 1.39 (2H, m, H-7), 1.35 (1H, m, H-15a), 1.29 (1H, m, H-9), 1.25 (1H, m, H-11b), 1.07 (3H, s, H-26), 1.03 (1H, m, H-12a), 1.01 (3H, s, H-27), 0.97 (3H, s, H-26), 0.97 (3H, s, H-23), 0.92 (1H, m, H-1a), 0.86 (3H, s, H-25), 0.85 (3H, s, H-25), 0.81 (3H, s, H-24), 0.78 (3H, s, H-23), 0.76 (3H, s, H-24), 0.72 (1H, m, H-5); ^{13}C NMR ($CDCl_3$, 125 MHz) δ: 179.7 (C-28), 152.2 (C-20), 110.8 (C-29), 78.9 (C-3), 57.5 (C-17), 56.1 (C-5), 50.5 (C-9), 49.2 (C-19), 46.9 (C-18), 42.3 (C-14), 40.7 (C-8), 38.8 (C-4), 38.7 (C-13), 38.7 (C-1), 37.1 (C-10), 37.0 (C-22), 34.4 (C-7), 32.3 (C-16), 30.4 (C-15), 29.7 (C-21), 28.0 (C-23), 27.9 (C-2), 25.3 (C-12), 20.9 (C-11), 19.6 (C-30), 18.4 (C-6), 15.9 (C-26), 15.8 (C-25), 15.4 (C-24), 15.0 (C-27).

Maslinic acid (**7**) – White powder. ^{1}H NMR (CD_3OD, 600 MHz) δ: 5.27 (1H, t, *J* = 3.6 Hz, H-12), 3.64 (1H, dt, *J* = 4.4, 10.6 Hz, H-2), 2.93 (1H, d, *J* = 10.6 Hz, H-3), 2.88 (1H, t, *J* = 4.8 Hz, H-18), 1.19 (3H, s, H-27), 1.03 (3H, s, H-25), 1.03 (3H, s, H-23), 0.96 (3H, s, H-30), 0.93 (3H, s, H-29), 0.84 (3H, s, H-24), 0.83 (3H, s, H-26); ^{13}C NMR (CD_3OD, 150 MHz) δ: 180.5 (C-28), 143.9 (C-13), 122.1 (C-12), 83.1 (C-3), 68.1 (C-2), 55.4 (C-5), 48.2 (C-9), 46.8 (C-1), 46.2 (C-17), 45.8 (C-19), 41.5 (C-18), 41.3 (C-14), 39.3 (C-4), 38.1 (C-8), 37.8 (C-10), 33.5 (C-21), 32.6 (C-7), 32.5 (C-22), 32.1 (C-29), 30.2 (C-20), 27.9 (C-23), 27.4 (C-15), 25.0 (C-27), 23.2 (C-11), 22.6 (C-30), 22.5 (C-16), 18.3 (C-6), 16.5 (C-26), 16.1 (C-24), 15.8 (C-25).

Arjungenin (**8**) – White powder. ^{1}H NMR (CD_3OD, 600 MHz) δ: 5.34 (1H, t, *J* = 3.76 Hz, H-12), 3.71 (1H, ddd, *J* = 4.5, 9.5, 11.4 Hz, H-2), 3.38 (1H, d, *J* = 9.5 Hz, H-3), 3.29 (1H, d, *J* = 9.5 Hz, H-23a), 3.54 (1H, d, *J* = 11.0 Hz, H-23b), 3.02 (1H, m, H-18), 3.28 (1H, m, H-19), 0.79–1.33 (18H, s, H-24, H-25, H-26, H-27, H-29, H-30); ^{13}C NMR (CD_3OD, 150 MHz) δ: 180.9 (C-28), 143.3 (C-13), 123.3 (C-12), 81.0 (C-19), 76.8 (C-3), 68.2 (C-2), 64.9 (C-23), 47.7 (C-9), 46.9 (C-5), 46.3 (C-1), 43.8 (C-18), 42.7 (C-4), 41.4 (C-14), 39.5.0 (C-8), 31.9 (C-7), 12.4 (C-24).

Aridanin (**9**) – White powder. ^{1}H NMR (CD_3OD, 400 MHz) δ: 8.53 (1H, s, NH), 5.99 (1H, brs, H-12), 5.06 (1H, d, *J* = 8.2 Hz, H-1′), 4.47 (1H, m, H-6′a), 4.24 (1H, m, H-3′), 4.23 (1H, m, H-6′b), 4.22 (1H, m, H-2′), 3.86 (1H, m, H-4′), 3.79 (1H, m, H-3), 3.78 (1H, m, H-5′), 2.1 (3H, s, N-Ac), 2.09 (1H, m, H-2a), 2.07 (1H, m, H-16), 2.03 (1H, m, H-22b), 1.82 (1H, m, H-22a), 1.75 (1H, m, H-2b), 1.18 (3H, s, H-27), 1.14 (3H, s, H-23), 1.09 (3H, s, H-30), 1.05 (3H, s, H-24), 0.99 (3H, s, H-26), 0.95 (3H, s, H-29), 0.79 (3H, s, H-25); ^{13}C NMR (CD_3OD, 100 MHz) δ: 179.9 (C-28), 170.3 (C-1′′), 145.0 (C-13), 122.8 (C-12), 104.8 (C-1′), 89.1 (C-3), 78.1 (C-5′), 76.2 (C-3′), 72.7 (C-4′), 62.9 (C-6′), 58.1 (C-2′), 55.7 (C-5), 47.8 (C-9), 46.7 (C-17), 46.5 (C-19), 42.2 (C-14), 41.9 (C-18), 39.5 (C-8), 39.2 (C-4), 38.6 (C-1), 36.8 (C-10), 34.2 (C-21), 33.7 (C-30), 33.3 (C-29), 33.3 (C-22), 33.1 (C-7), 30.9 (C-20), 28.2 (C-23), 28.2 (C-15), 26.3 (C-2), 26.2 (C-27), 23.8 (C-16), 23.7 (C-11), 23.6 (C-2′′), 18.4 (C-6), 17.4 (C-26), 16.8 (C-24), 15.6 (C-25).

Hederagenin-3-*O*-*α*-L-arabinopyranoside (**10**) – White powder. ^{1}H NMR (CD_3OD, 500 MHz) δ: 5.26 (1H, t, *J* = 3.7 Hz, H-12), 4.33 (1H, d, *J* = 6.8 Hz, H-1′), 3.86 (1H, dt, *J* = 12.4, 2.4 Hz, H-5′a), 3.81 (1H, dt, *J* = 4.4, 2.0 Hz, H-3′), (3.62 (1H, m, H-3), 3.62 (1H, m, H-23a), 3.56 (1H, m, H-5′b), 3.55 (1H, m, H-2′), 3.51 (1H, dd, *J* = 9.0, 3.3 Hz, H-4′), 3.30 (1H, m, H-23b), 2.86 (1H, dd, *J* = 13.7, 4.1 Hz, H-18), 2.03 (1H, m, H-16b), 2.03 (1H, m, H-16a), 1.79 (1H, m, H-15a), 1.65 (1H, m, H-9), 1.52 (1H, m, H-22a), 1.40 (1H, m, H-21a), 1.39 (1H, m, H-22b), 1.27 (1H, m, H-5), 1.22 (1H, m, H-21b), 1.19 (3H, s, H-27), 1.16 (1H, m, H-19a), 1.12 (1H, m, H-19b), 1.09 (1H, m, H-15b), 1.00 (3H, s, H-25), 0.96 (3H, s, H-29), 0.93 (3H, s, H-30), 0.83 (3H, s, H-26), 0.73 (3H, s, H-24); ^{13}C NMR (CD_3OD, 125 MHz) δ: 180.0 (C-28), 143.8 (C-13), 122.1 (C-12), 104.9 (C-1′), 81.7 (C-3), 73.1 (C-4′), 71.6 (C-2′), 68.3 (C-3′), 65.4 (C-5′), 63.4 (C-23), 47.6 (C-9), 46.7 (C-5), 45.7 (C-19), 42.4 (C-4), 41.5 (C-14), 41.3 (C-18), 39.1 (C-8), 38.0 (C-1), 36.2 (C-10), 33.4 (C-21), 32.1 (C-7), 32.1 (C-6), 30.1 (C-20), 27.4 (C-15), 24.9 (C-27), 22.5 (C-29), 22.5 (C-16), 20.6 (C-17), 17.4 (C-22), 16.3 (C-30), 16.3 (C-26), 14.9 (C-25), 11.9 (C-24).

Ursolic acid (**11**) - White powder. ^{1}H NMR (DMSO-*d6*, 500 MHz) δ: 5.15 (1H, d, *J* = 12.0 Hz, H-12), 2.90 (1H, dd, *J* = 12.0, 6.0 Hz, H-3), 1.80 (1H, m, H-19), 1.74 (2H, m, H-22), 1.49 (1H, m, H-20), 1.31 (3H, s, H-27), 1.25 (3H, d, *J* = 6.0 Hz, H-29), 1.23 (3H, d, *J* = 6.0 Hz, H-30), 1.15 (3H, s, H-23), 1.10 (3H, s, H-25), 1.02 (3H, s, H-26), 0.98 (3H, s, H-24); ^{13}C NMR (DMSO-*d6*, 125 MHz) δ: 178.8 (C-28), 138.6 (C-13), 125.0 (C-12), 77.3 (C-3), 55.2 (C-5), 52.8 (C-18), 48.9 (C-17), 47.4 (C-9), 42.0 (C-14), 41.7 (C-8), 38.9 (C-4), 38.8 (C-19), 38.7 (C-20), 38.6 (C-1), 36.9 (C-22), 36.7 (C-10), 33.1 (C-7), 30.6 (C-21), 28.6 (C-15), 27.9 (C-23), 27.2 (C-2), 26.0 (C-16), 24.2 (C-27), 23.7 (C-11), 21.5 (C-30), 18.4 (C-6), 17.4 (C-26), 17.3 (C-29), 16.5 (C-24), 15.6 (C-25).

Tormentic acid (**12**) – White powder. ^{1}H NMR (Pyridine-d_5, 500 MHz) δ: 5.56 (1H, brs, H-12), 4.07 (1H, m, H-2), 3.37 (1H, d, *J* = 9.5 Hz, H-3), 3.10 (1H, m, H-16), 3.03 (1H, s, H-18), 1.68 (3H, s, H-27), 1.40 (3H, s, H-29), 1.25 (3H, s, H-23), 1.19 (3H, s, H-30), 1.09 (3H, s, H-26), 1.05 (3H, s, H-24), 0.97 (3H, s, H-25); ^{13}C NMR (Pyridine-d_5, 150 MHz) δ: 180.7 (C-28), 139.7 (C-13), 128.2 (C-12), 83.6 (C-3), 72.4 (C-19), 68.3 (C-2), 55.7 (C-5), 54.3 (C-18), 48.0 (C-17), 47.7 (C-9), 47.6 (C-1), 42.1 (C-20), 41.9 (C-14), 40.2 (C-8), 39.6 (C-4), 38.5 (C-22), 38.5 (C-10), 31.4 (C-7), 29.1 (C-23), 29.1 (C-15), 26.8 (C-29), 26.7 (C-21), 26.1 (C-16), 24.4 (C-27), 23.9 (C-11), 18.8 (C-6), 17.4 (C-24), 17.2 (C-26), 16.6 (C-25), 16.5 (C-30).

Taraxeryl acetate (**13**) – White crystals. ^{1}H NMR ($CDCl_3$, 400 MHz) δ: 5.56 (1H, *J* = 8.2, 3.2 Hz, H-15), 4.49 (1H, *J* = 11.1, 5.0 Hz, H-3), 2.01 (3H, s, H-2′), 2.01 (1H, m, H-16b), 1.95 (1H, m, H-16a), 1.75 (1H, m, H-2a), 1.67 (1H, m, H-7a), 1.63 (1H, m, H-6a), 1.60 (1H, m, H-1a), 1.42 (1H, s, H-9), 1.42 (1H, m, H-7b), 1.40 (1H, m, H-18), 1.40 (1H, m, H-1b), 1.38 (1H, m, H-6b), 1.31 (1H, m, H-2b), 1.19 (2H, m, H-11), 1.17 (2H, m, H-12), 1.15 (2H, m, H-22), 1.15 (2H, m, H-19), 1.14 (2H, m, H-21), 1.12 (3H, s, H-26), 1.10 (3H, s, H-27), 0.99 (3H, s, H-28), 0.99 (3H, s, H-25), 0.94 (3H, s, H-24), 0.94 (1H, m, H-5), 0.92 (3H, s, H-23), 0.84 (3H, s, H-29), 0.83 (3H, s, H-30); ^{13}C NMR ($CDCl_3$, 100 MHz) δ: 171.0 (C-1′), 158.0 (C-14), 117.0 (C-15), 81.0 (C-3), 55.7 (C-5), 49.2 (C-9), 48.8 (C-18), 41.2 (C-19), 39.0 (C-8), 37.9 (C-4), 37.7 (C-13), 37.7 (C-1), 37.6 (C-10), 37.4 (C-22), 36.7 (C-12), 35.7 (C-17), 35.1 (C-21), 33.7 (C-16), 33.4 (C-29), 33.1 (C-7), 29.9 (C-27), 29.7 (C-28), 28.8 (C-20), 28.0 (C-23), 26.0 (C-26), 23.5 (C-2), 21.4 (C-2′), 21.3 (C-30), 18.7 (C-6), 17.5 (C-11), 16.6 (C-24), 15.5 (C-25).

Rhaponticin (**14**) – Brown powder. ^{1}H NMR (C_5D_5N, 600 MHz) δ: 7.03 (1H, d, J = 2.0 Hz, H-2′), 6.94 (1H, d, J = 16.1 Hz, H-β), 6.91 (1H, dd, J = 8.1, 2.0 Hz, H-6′), 6.81 (1H, d, J = 16.1 Hz, H-α), 6.78 (1H, d, J = 8.1 Hz, H-5′), 6.76 (1H, brs, H-2), 6.59 (1H, brs, H-6), 6.48 (1H, dd, J = 1.8, 2.2 Hz, H-4), 4.92 (1H, d, J = 7.3 Hz, H-1′′), 4.63 (1H, dd, J = 12.1, 2.2 Hz, H-6′′a), 4.31 (1H, dd, J = 12.1, 7.7 Hz, H-6′′b), 3.83 (1H, m, H-5′′), 3.80 (3H, s, 4′–OCH_3), 3.52 (2H, m, H-2′′,H-3′′), 3.39 (1H, dd, J = 9.1, 7.9 Hz, H-4′′); ^{13}C NMR (C_5D_5N, 150 MHz) δ: 160.3 (C-5), 160.3 (C-3), 148.8 (C-4′), 147.4 (C-3′), 140.6 (C-1), 131.4 (C-1′),129.6 (C-β), 127.2 (C-α), 118.9 (C-6′), 113.4 (C-2′), 112.4 (C-5′), 108.7 (C-6), 105.9 (C-2), 103.1 (C-4), 100.5 (C-1′′), 76.5 (C-3′′), 76.1 (C-5′′), 75.1(C-2′′), 71.24 (C-4′′), 62.3 (C-6′′), 55.8 (4′–OCH_3)

Stigmasterol (**15**) – White powder. ^{1}H NMR ($CDCl_3$, 500 MHz) δ : 5.36 (1H, t, J = 6.2, H-6), 5.14 (1H, dd, J = 12.3, 8.0 Hz, H-22), 4.98 (1H, dd, J = 12.3, 8.0 Hz, H-23), 3.53 (1H, dd, J = 4.3, 4.1 Hz, H-3), 1.03 (3H, s, H-19), 0.93 (3H, s, H-18), 0.87 (1H, t, J = 7.2 Hz, H-24), 0.84 (3H, d, J = 6.6 Hz, H-26), 0.82 (3H, t, J = 6.5 Hz, H-29), 0.81 (3H, d, J = 6.6 Hz, H-27), 0.71 (3H, d, J = 6.3 Hz, H-21); ^{13}C NMR ($CDCl_3$, 125 MHz) δ: 140.8 (C-5), 138.3 (C-22), 129.3 (C-23), 121.7 (C-6), 71.8 (C-3), 56.9 (C-14, C-17), 51.3 (C-24), 50.2 (C-9), 42.4 (C-4, C-13), 40.5 (C-20), 39.8 (C-12), 37.3 (C-1), 36.6 (C-10), 32.0 (C-7), 31.9 (C-8), 31.7 (C-2), 31.2 (C-25), 28.9 (C-16), 25.4 (C-28), 24.4 (C-15), 21.2 (C-26, C-27), 21.1 (C-11, C-21), 19.4 (C-19), 12.2 (C-18, C-29)

Stigmasterol-3-*O*-β-D-glucopyranoside (**16**) – White powder. ^{1}H NMR (C_5D_5N, 500 MHz) δ: 5.32 (2H, m, H-6), 5.16 (1H, dd, J = 12.1, 8.2 Hz, H-22), 5.03 (1H, dd, J = 12.1, 8.2 Hz, H-23), 4.22 (1H, d, J = 6.5 Hz, H-1′), 3.67 (1H, m, H-6′b), 3.47 (1H, m, H-3), 3.44 (1H, m, H-6′a),3.12 (1H, d, J = 7.5 Hz, H-3′), 3.10 (1H, m, H-5′), 3.06 (1H, m, H-4′), 2.90 (1H, t, J = 7.0 Hz, H-2′), 2.12 (1H, m, H-20), 1.93 (2H, m, H-4), 1.80 (4H, m, H-15, H-16), 1.80 (2H, m, H-7), 1.63 (1H, m, H-27), 1.50 (6H, m, H-8, H-9, H-11, H-12), 1.50 (4H, m, H-24, H-26), 1.39 (2H, m, H-2), 1.24 (2H, m, H-1), 1.24 (1H, m, H-17), 1.15 (2H, m, H-25), 1.15 (1H, m, H-14), 0.99 (3H, d, J = 6.9 Hz, H-29), 0.95 (3H, s, H-19), 0.90 (3H, d, J = 6.4 Hz, H-21), 0.82 (3H, s, H-18), 0.76 (3H, m, H-28); ^{13}C NMR (C_5D_5N, 125 MHz) δ: 141.0 (C-5), 138.8 (C-22), 129.6 (C-23), 121.9 (C-6), 102.6 (C-1′), 78.6 (C-3), 78.4 (C-3′), 78.2 (C-5′), 75.4 (C-2′), 71.8 (C-4′), 63.0 (C-6′), 57.0 (C-14), 56.2 (C-17), 51.5 (C-24), 50.4 (C-9), 42.4 (C-4, C-13), 40.8 (C-20), 39.4 (C-12), 37.5 (C-1), 37.0 (C-10), 32.2 (C-2, C-7), 32.1 (C-8, C-25), 29.3 (C-16), 25.7 (C-28), 24.6 (C-15), 21.3 (C-21), 19.5 (C-11, C-26), 19.3 (C-27), 19.2 (C-19), 12.5 (C-29), 12.2 (C-18)

3.3. Antiplasmodial activity

The main goal of this study was to provide further evidence which might justify or support the use of the plant *T. tetraptera* in traditional medicine for the treatment of malaria. After extraction of the stem bark and roots using methanol, the obtained crude extracts were screened for their potential antiplasmodial activity against the chloroquine-sensitive strain *P. falciparum* 3D7. The results demonstrated that both extracts significantly inhibit the parasite growth at 10 μg/ml with the rates of 83.6% and 76.3%, respectively. This result encouraged the chemical investigations of both extracts to isolate their specialized metabolites that might be responsible for the activity. A total of sixteen compounds (Fig. 1) have been obtained among which thirteen (compounds **2–9, 11–13, 15** and **16**) were further evaluated for their antiplasmodial activity using chloroquine as reference drug and the results are compiled in Table 2. In our recent review on the antiplasmodial activity of compounds from the Meliaceae plant family, we reported the five categories of antiplasmodial compounds in their classification based on their IC_{50} value ranges which classified a pure compound as an active one by the industry if its IC_{50} value is lower than 10 μM established as standard value (Happi et al., 2022). From that scale, ten compounds over the thirteen tested ones can be considered as active compounds with IC_{50} < 10 μM including (in order of potency) betulin (**5**) and aridanin (**9**) which were the most active with IC_{50} values of (1.8 ± 0.4 μM) and (1.9 ± 0.8 μM), respectively, followed by maslinic acid (**7**), butein (**2**) and betulinic acid (**6**) which displayed IC_{50} values of (2.1 ± 0.5 μM), (2.3 ± 0.7 μM), (2.4 ± 0.6 μM), respectively. Additionally, three additional compounds namely 3β-taraxeryl acetate (**13**) (IC_{50} = 4.2 ± 1.3 μM), lupeol (**3**) (IC_{50} = 4.4 ± 0.8 μM) and tormentic acid (**12**) (IC_{50} = 4.8 ± 1.5 μM) showed good activities with IC_{50} > 0.1 μM but ≤ 5 μM, while lupenone (**4**) and stigmasterol-3-*O*-β-D-glucopyranoside (**16**) showed moderate activity with IC_{50} values of (5.7 ± 1.1) μM and 6.7 ± 1.8) μM, respectively. Finally, arjungenin (**8**) and ursolic acid (**11**) demonstrated a weak activity with IC_{50} values of (26.1 ± 2.2) μM and (36.2 ± 2.3) μM, respectively, whereas stigmasterol (**15**) was inactive (IC_{50} = 102.3 ± 14.6 μM).

Table 2
Antiplasmodial activity against Pf 3D7 and binding energy to the anti-plasmodium (5TBO) receptor.

Compounds	IC_{50} (μM)	Binding Energy (ΔG) kcal/mol
1	n.t	−8.7
2	2.3 ± 0.7	−8.9
3	4.4 ± 0.8	−8.8
4	5.7 ± 0.7	−8.8
5	1.8 ± 0.4	−8.0
6	2.4 ± 0.6	−8.2
7	2.1 ± 0.5	−8.3
8	36.2 ± 0.3	−8.2
9	1.9 ± 0.8	−8.0
10	n.t	−8.4
11	26.1 ± 0.2	−8.6
12	4.8 ± 0.5	−8.2
13	4.2 ± 0.3	−8.9
14	n.t	−9.3
15	102.3 ± 2.6	−8.7
16	6.7 ± 0.8	−8.6
Chloroquine	0.08 ± 0.01	−7.3

n.t: not tested.

From these results, a tentative elaboration of the action mechanism of the isolated compounds has been done. The three lupane-type triterpenoids (**3–6**) displayed different activities that might be related to the nature of the functional groups at positions 3 and 28 in the main carbon chain of the compounds. For instance, the results showed that betulin (**5**) is the most active compared to the other lupane-triterpenoids, and there is also a decrease in the activity when moving from lupeol (**3**) to its derivative lupenone (**4**) indicating that the presence of hydroxyl group at positions 3 and 28 might play an important role in the increasing of the antiplasmodial activity of lupane-type triterpenoids.

Likewise, the antiplasmodial evaluation of the three oleanane-type triterpenoids (**7–9**) led to the observation that maslinic acid (**7**) and aridanin (**9**) showed similar good activities while arjungenin (**8**) was not active. From their structural consideration, it seems obvious that substitution of a sugar moiety at C-3 of the structure might be favourable to improve their activity, while the oxidation of Me-23 to CH_2OH and the presence of a hydroxyl group at C-19 might exert an antagonistic effect on the potency of oleanane-triterpenoids.

Finally, we also observed that stigmasterol-3-*O*-β-D-glucopyranoside (**16**) is more than fifteen times more active than its congener stigmasterol (**15**). As partially concluded for compounds **7–9**, the presence of the glucoside moiety at C-3 in compound **16** can justify the high increase in its activity compared to compound **15**. Therefore, sugar moiety can play an important role in the improvement of the antiplasmodial activity of triterpenoids and steroids. Further insights into understanding the action mechanisms of the tested active compounds have been provided by the molecular docking of the compounds.

3.4. Molecular docking

Along the journey in developing new approaches to fighting malaria, it has been found that dihydroorotate dehydrogenase is an important target enzyme of *Plasmodium* associated with the strain *P. falciparum* 3D7 (the strain for the in vitro tests) and which can be bound with the selective inhibitor DSM421 as a ligand to form the receptor reported under the PDB code 5TBO (Phillips et al., 2016). All the sixteen compounds isolated from *Tetrapleura tetraptera* as well as the selected standard (chloroquine) have been computationally evaluated for their binding affinities with the 5TBO receptor (Table 2 and Figs. 2-7). From the results obtained, all the compounds displayed greater affinity than chloroquine (Table 2). These results were in agreement with the in vitro antiplasmodial tests using *P. falciparum* 3D7 which suggested that the plant *T. tetraptera* has a resounding capacity as a potential anti-plasmodium therapeutic.

Five compounds (**2, 5, 6, 7** and **9**) were found significantly in vitro active with IC_{50} values lower than 5 μM. Close observation of their binding affinity and docking poses provided additional information on their inhibition mechanisms of the *Plasmodium* parasite. The most active compound **5** and its congener **6** displayed close binding affinities (energies) and the same interactions with the receptor 5TBO, mostly presented as a residue-hydrogen bond interaction with LYS229 (5.25 and 5.27). Similar interactions were observed for the active compounds **7** and **9** presenting conventional hydrogen bonds with LYS229 (5.26) and THR249 (2.93) for **7**, as well as THR249 (2.76), LYS429 (2.51) and ASN258 (2.76) for **9**. Finally, compound **2** indicated important residue-hydrogen bond interactions with SER505 (1.96), ILE508 (2.33) and CYS530 (2.93).

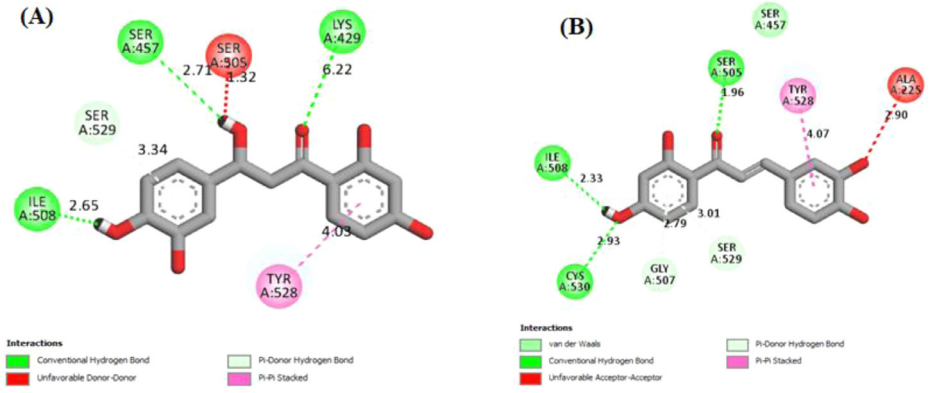


Fig. 2. Interaction at the 5TBO receptor binding site for compounds **1** (A) and **2** (B).

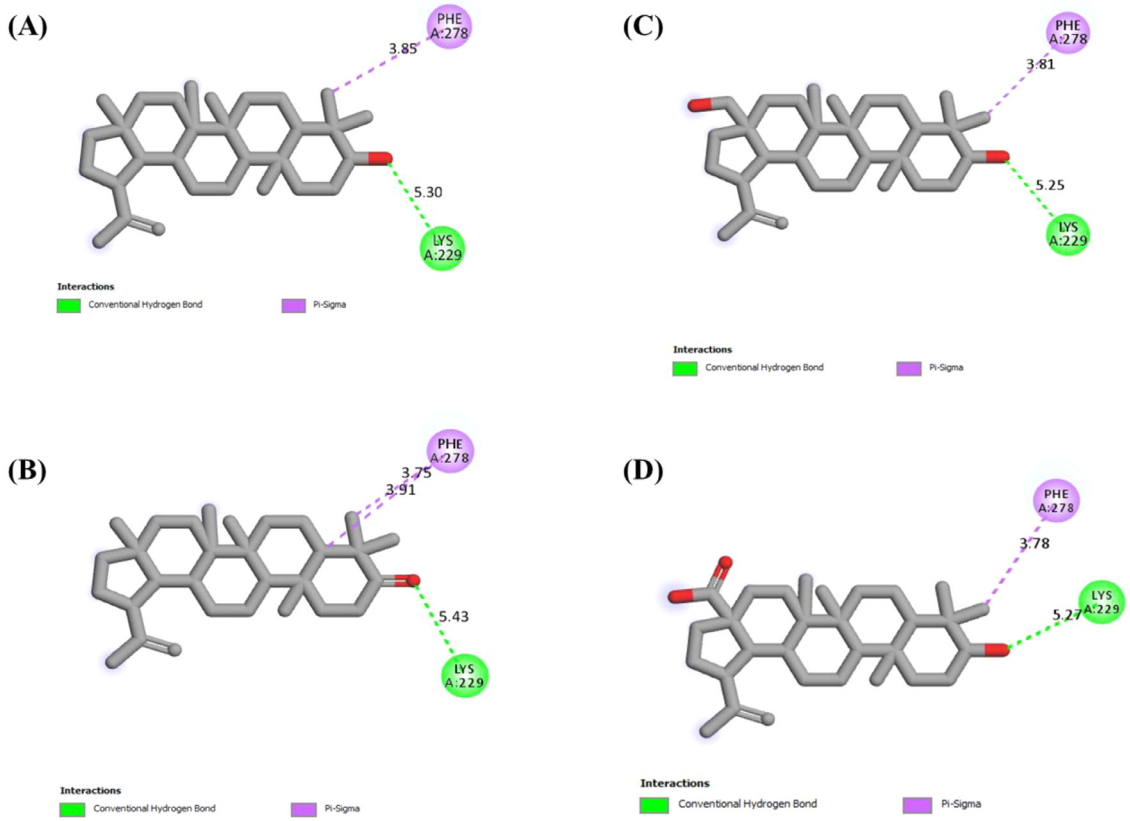


Fig. 3. Interaction at the 5TBO receptor binding site for compounds **3** (A), **4** (B), **5** (C) and **6** (D).

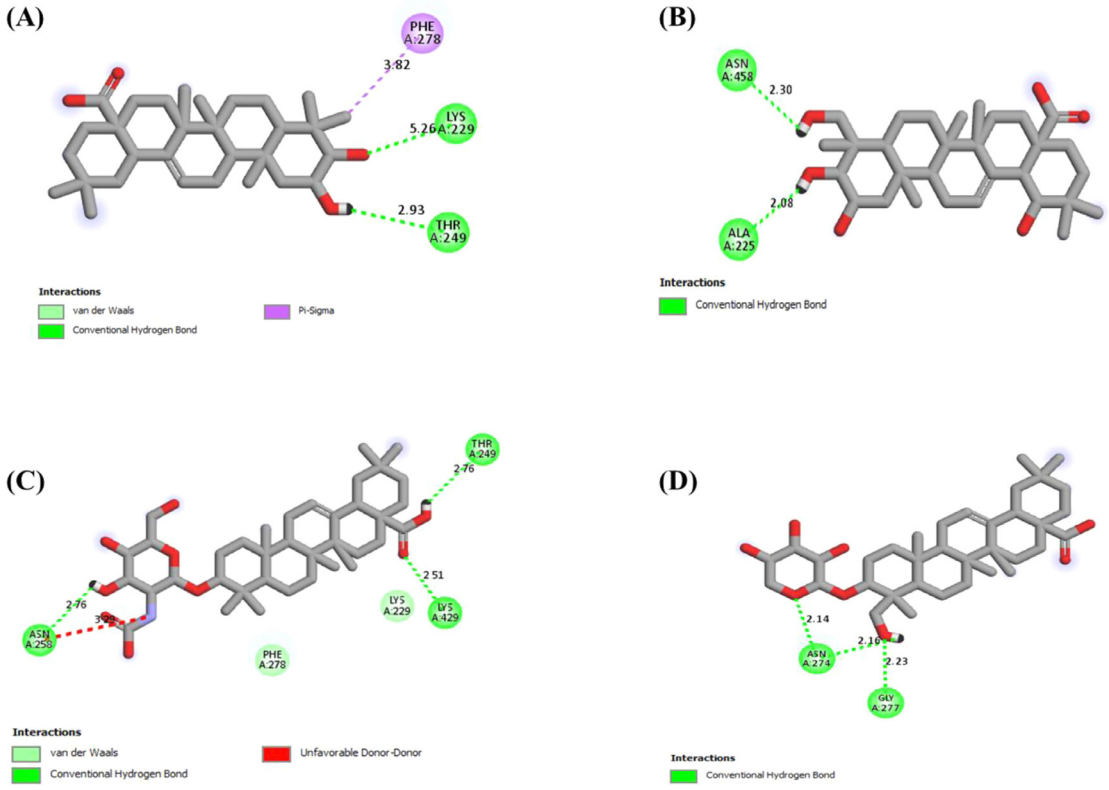


Fig. 4. Interaction at the 5TBO receptor binding site for compounds **7** (A), **8** (B), **9** (C) and **10** (D).

We also found that compound **15** was more than fifteen times less active than its glycosylated derivative **16**. Observation of their docking poses with the receptor's binding site showed one interaction between the glucoside unit of compound **16** through a conventional hydrogen bond with GLY474 (2.48). We can partially conclude in waiting for further analyses that the amino acids LYS229, THR249 and GLY474 might play a key role in the inhibition mechanism of the *Plasmodium* enzyme dihydroorotate dehydrogenase.

It can also be mentioned that since chloroquine, the standard drug used for this study resulted in a maximum number of 2 conventional hydrogen bonds (Fig. 7) while most selected compounds exhibited more, and with shorter bond length, it is understandable why the identified compounds have greater binding affinity to the anti-plasmodium receptor than the standard.

3.5. ADMET studies

The ADMET prediction results are shown in Table 3. The human intestinal absorption (HIA) of an oral drug is the essential prerequisite for its apparent efficacy. What is more, the close relationship between oral bioavailability and intestinal absorption has also been proven and HIA can be seen as an alternative indicator for oral bioavailability to some extent. A drug molecule with an absorbance of less than 30% is poorly absorbed (Xiong et al., 2021). Results from Table 3 shows that compounds **1**–**4, 7**–**8, 10**–**11, 13, 15** and chloroquine agree to be strongly absorbed by the intestine.

Water solubility is one important condition a drug must satisfy before in vitro drug optimization process (Xiong et al., 2021). Results show that all identified compounds are more water soluble with **3** (−6.667), **4** (−6.605), **13** (−6.689), **15** (−7.008) being very soluble than the selected standard chloroquine (−3.902).

Cytochrome CYP450 inhibitors are responsible for the biotransformation of a drug; a potential drug should not alter their kinetics (Sanguinetti et al., 2006). Results shows that none of the selected compounds inhibited the cytochrome receptors greater than chloroquine (2/5).

The Human either-a-go-go related inhibition (hERG) is a measure of electrical pulse transmission in the human heart (iodine-

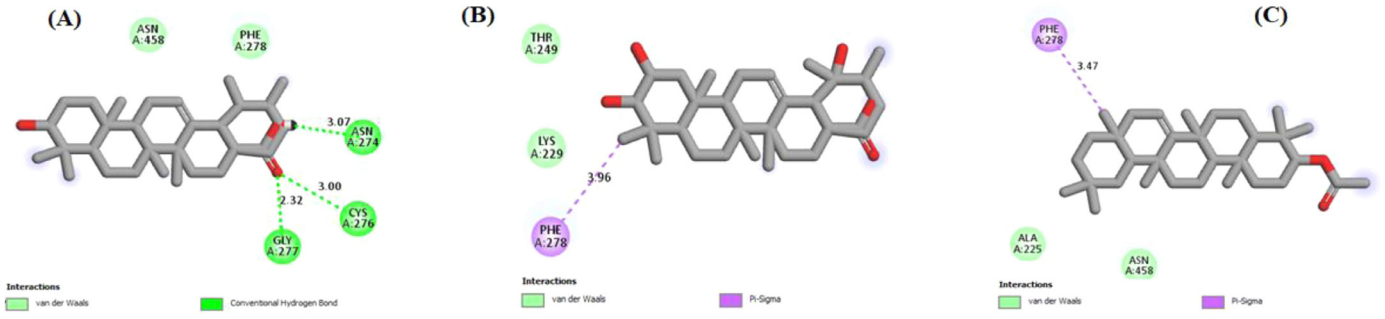


Fig. 5. Interaction at the 5TBO receptor binding site for compounds **11** (A), **12** (B) and **13** (C).

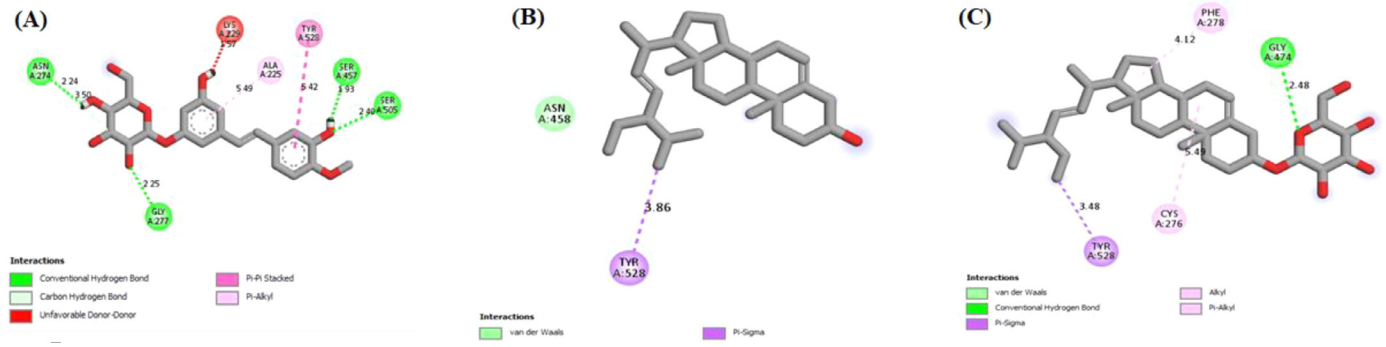


Fig. 6. Interaction at the 5TBO receptor binding site for compounds **14** (A), **15** (B) and **16** (C).

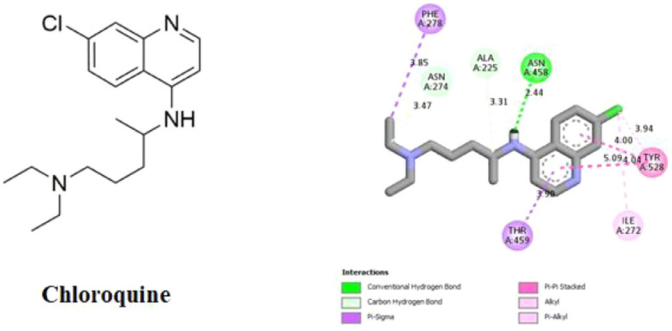


Fig. 7. Chemical structure of chloroquine and its interaction at the 5TBO receptor binding site.

channel blocking). A potential drug should not block the activity of the hERG inhibitors (Sanguinetti et al., 2006). Table 3 shows that all compounds present themselves as inactive against blocking the heart functions, as the standards. Carcinogenicity results also show that none of the identified compounds are a direct poison.

Brain Blood Barrier (BBB) prediction test suggest that compounds **1–2, 7–8, 10–11, 13–15** do not have ability to cross the BBB, hence their mode of action do not involve neurological engineering, such as appetite reduction as in chloroquine. It also suggests that the nine compounds will pose little or no side effects on administration as compared to chloroquine.

A good drug must also be able to stay long (activity) enough in the body before excretion. The half-life of a drug is the description of how long a drug will stay active for in the body before excretion. The results in Table 3 indicate that compounds **1, 2**, and **14** of the selected will stay long enough twice longer than chloroquine. Furthermore, results show that compounds **4** and **8** will also stay longer than the standard drugs but with a time shorter than for compounds **1, 2** and **14**.

Table 3 also describes the drug likeliness based on Lipinski rules of five (Lipinski, 2001) : The rule states that a compound that must stand as a potential drug, its structural properties must first satisfy the following rules: Molecular weight $\leq$ 500, MiLOGP $\leq$ 4.15, Number of oxygen $\leq$ 10, Number of hydrogen $\leq$ 5, Number of hydroxide $\leq$ 5.

Table 3
ADMET score of qualified compounds from *T. tetraptera*, with respect to the selected standards.

Compounds	HIA	BBB	Water solubility (mol/L)	CYP450 inhibition	hERG inhibition	Drug likeness (Lipinski)	$T_{(1/2)}$	Carcinogenicity
1	Yes (> 60%)	No	soluble (−3.615)	1/5	Inactive	Yes (5/5)	Long (0.868)	No
2	Yes (> 90%)	No	soluble (−2.993)	2/5	Inactive	Yes (5/5)	Long (0.924)	No
3	Yes (> 90%)	Yes	Very soluble (−6.667)	0/5	Inactive	Yes (5/5)	Very short 0.037	No
4	Yes (> 90%)	Yes	Very soluble (−6.605)	0/5	Inactive	Yes (5/5)	Short 0.109	No
7	Yes (> 90%)	No	Soluble (−4.943)	0/5	Inactive	Yes (5/5)	Very short (0.052)	No
8	Yes (> 90%)	No	Soluble (−3.829)	0/5	Inactive	Yes (5/5)	Short (0.122)	No
10	Yes (> 60%)	No	Soluble (−3.498)	0/5	Inactive	Yes (5/5)	Very short (0.041)	No
11	Yes (> 90%)	No	Soluble (−4.479)	0/5	Inactive	Yes (5/5)	Very short (0.029)	No
13	Yes (>90%)	No	Very soluble (−6.689)	0/5	Inactive	Yes (5/5)	Very short (0.049)	No
14	No (< 30%)	No	Soluble (−3.098)	1/5	Inactive	Yes (5/5)	Long (0.812)	No
15	Yes (> 90%)	No	Very soluble (−7.008)	1/5	Inactive	Yes (5/5)	Very short (0.030)	No
Chloroquine	Yes (>90%)	Yes	Soluble (−3.902)	2/5	Inactive	Yes (5/5)	Very short (0.070)	No

Results show that all identified compounds satisfy this drug condition and hence are more likely than unlikely to be applied as a drug.

4. Conclusion

The chemical studies of the stem bark and root of *Tetrapleura tetraptera* led to the identification of sixteen (**1**–**16**) compounds among which thirteen have been tested for their antiplasmodial activity to identify the lead compounds responsible for the activity of the extracts. The results of biotests showed that ten compounds (**2**–**7, 9, 12, 13, 16**) possess good activity with $IC_{50} < 10\ \mu M$ and the most potent ones were compounds **5, 9, 7, 2** and **6** with IC_{50} values of $(1.8 \pm 0.4\ \mu M)$, $(1.9 \pm 0.8\ \mu M)$, $(2.1 \pm 0.5\ \mu M)$, $(2.3 \pm 0.7\ \mu M)$, $(2.4 \pm 0.6\ \mu M)$, respectively. The docking analyses of the active compounds led to the partial conclusion that the bond lengths and the amino acids LYS229, THR249 and GLY474 in the 5TBO receptor's binding site might play an important role in the inhibition mechanism of the *Plasmodium* parasite while butein (**2**) and compounds **1, 4, 8** and **14** demonstrated great ability in drug development. The present study classifies *T. tetraptera* as an important source of good candidates in antiplasmodial drug development, supports its use in traditional medicine for the management of malaria and related symptoms and gives further details on the identification of lead compounds from the plant, their possible action mechanism as well as their ability to be developed as drugs. As an extension of the scope of this study, the chemical modifications of active compounds might lead to an improvement of their potency while their quantification will help in knowing the proportion of active principles in the extracts. Furthermore, the evaluation of the toxicity of the extracts and pure active compounds will be necessary on the way forward in formulating potent and less toxic phytomedicines or new discovering new antimalarial drugs for the local population.

Declaration of Competing Interest

The authors declare that they have no conflicts of interest.

References

Abouelela, M.E., Orabi, M.A.A., Abdelhamid, R.A., Abdelkader, M.S.A., Darwish, F.M.M., 2018. Chemical and cytotoxic investigation of non-polar extract from *Ceiba pentandra* (L.) Gaertn.: a study supported by computer based screening. J. Appl. Pharmaceut. Sci. 8, 57–64.

ACD/ChemSketch, 2020. *Advanced Chemistry Development*, Inc., Toronto, ON, Canada. [Online]. Available: www.acdlabs.com.

Adesina, S.K., Iwalewa, E.O., Johnny, I.I., 2016. *Tetrapleura tetraptera* Taub - Ethnopharmacology, chemistry, medicinal and nutritional values a review. British J. Pharmaceut. Res. 12, 1–22.

Adesina, S.K., Reisch, J., 1985. A triterpenoid glycoside from *Tetrapleura tetraptera* fruit. Phytochemistry 24, 3003–3006.

Adewunmi, C.O., 1993. Control of snail intermediate hosts in schistosomiasis review. Nig. J. Parasitol. 14, 45–51.

Ahmadu, A.A., Delehouze, C., Haruna, A., Mustapha, L., Lawal, B.A., Udobre, A., Baratte, B., Triscornia, C., Autret, A., Robert, T., Bulinski, J.C., Rousselot, M., Eugenio, M.S., Dimanche-Boitrel, M.-T., Petzer, J.P., Legoabe, L.J., Bach, S., 2021. Betulin, a newly characterized compound in *Acacia auriculiformis* bark, is a multi-target protein kinase inhibitor. Molecules 26, 4599. https://doi.org/10.3390/molecules26154599.

An, H.-J., Kim, I.-T., Park, H.-J., Kim, H.-M., Choi, J.-H., Lee, K.-T., 2011. Tormentic acid, a triterpenoid saponin, isolated from *Rosa rugosa*, inhibited LPS-induced iNOS, COX-2, and TNF-α expression through inactivation of the nuclear factor-κb pathway in RAW 264.7 macrophages. Int. Immunopharmacol. 11, 504–510.

Biovia, D., 2021. BIOVIA Workbook. Dassault Systèmes, San Diego. Release 2021; BIOVIA Pipeline Pilot, Release.

Bongmo, L.V.L., Nouga, A.B., Happi, G.M., Tabekoueng, G.B., Lateef, M., Waffo, A.F.K., Ali, M.S., Choudhary, M.I., Wansi, J.D., 2022. Phytochemical compounds of *Guibourtia ehie* and their antioxidant, urease and α-glucosidase inhibitory activities. Nat. Res. Human Health 2, 306–312.

Bukvicki, D., Gottardi, D., Prasad, S., Novakovic, M., Marin, D., Tyagi, A., 2020. The healing effects of spices in chronic diseases. Curr. Med. Chem. 27, 4401–4420.

Burkill, H.M., 1995. The Useful Plants of West Tropical Africa, 2nd ed. Royal Botanic Gardens, Kew, pp. 263–265.

Cheng, F., Li, W., Zhou, Y., Shen, J., Wu, Z., Liu, G., Lee, P.W., Tang, Y., 2012. admetSAR: a comprehensive source and free tool for assessment of chemical ADMET properties. J. Chem. Inform. Model. 52, 3099–3105.

Daina, A., Michielin, O., Zoete, V., 2017. SwissADME: a free web tool to evaluate pharmacokinetics, drug-likeness and medicinal chemistry friendliness of small molecules. Sci. Rep. 7, 42717.

Dalziel, J.M., 1955. The Useful Plants of West Tropical Africa. Crown Agents for Overseas Governments and Administrations, pp. 223–224.

Falade, V.A., Adelusi, T.I., Adedotun, I.O., Abdul-Hammed, M., Lawal, T.A., Agboluaje, S.A., 2021. In silico investigation of saponins and tannins as potential inhibitors of SARS-CoV-2 main protease (Mpro). In Silico Pharmacol 9, 9–15.

Ghosh, A.K., Banerjee, S., Mullick, H.I., Banerjee, J., 2011. *Zingiber officinale*: a natural gold. Int. J. Pharm. Biol. Sci. 2, 283–294.

Happi, G.M., Kouam, S.F., Talontsi, F.M., Lamshöft, M., Zühlke, S., Bauer, J.O., Strohmann, C., Spiteller, M., 2015. Antiplasmodial and cytotoxic triterpenoids from the bark of the Cameroonian medicinal plant *Entandrophragma congoënse*. J. Nat. Prod. 78, 604–614.

Happi, G.M., Mbobda, A.S.W., Frese, M., Kouam, S.F., Tchouankeu, J.C., Lenta, B.N., Sewald, N., 2021. A new phenylpropanoid glycoside from *Psorospermum tenuifolium* Kotschy (Hypericaceae). Trends Phytochem. Res. 5, 31–36.

Happi, G.M., Nangmo, P.K., Dzouemo, L.C., Kache, S.F., Kouam, A.D.K., Wansi, J.D., 2022. Contribution of Meliaceous plants in furnishing lead compounds for antiplasmodial and insecticidal drugs development. J. Ethnopharmacol. 285, 114906.

Happi, G.M., Wouamba, S.C.N., Ismail, M., Kouam, S.F., Frese, M., Lenta, B.N., Sewald, N., 2020. Ergostane-type steroids from the Cameroonian 'white tiama' *Entandrophragma angolense*". Steroids 156, 108584.

Honda, T., Murae, T., Tsuyuki, T., Takahashi, T., 1976. The structure of arjungenin. A new sapogenin from *Terminalia arjuna*. Chem. Pharm. Bull. 24, 178–180.

Irvine, F.R., 1961. Woody Plants of Ghana with Special Reference to Their Uses. Oxford University Press, London, p. 58.

Jhoo, J.-W., Sang, S., He, K., Cheng, X., Zhu, N., Stark, R.E., Zheng, Q.Y., Rosen, R.T., Ho, C.-T., 2021. Characterization of the triterpene saponins of the roots and rhizomes of blue Cohosh (*Caulophyllum thalictroides*). J. Agri. Food Chem. 49, 5969–5974.

Kemayou, G.P.M., Happi, G.M., Ngandjui, Y.A.T., Tchouankeu, J.C., Sewald, N., Ali, M.S., Kouam, S.F., 2020. Senegalin, a new phenylpropanoid and other secondary metabolites from the stem bark of *Ekebergia senegalensis* A. Juss. (Meliaceae). Nat. Prod. Res. 35, 3694–3700.

Kemigisha, E., Edmund, O., Christinah, A., Francis, O., Paul, P.B., 2018. *Tetrapleura tetraptera* in Ghana, Nigeria and Uganda: households used and local market. Forests. Trees and Livelihoods 27, 243–256.

Keugwa, C.V.T., Ehawa, F.R.E., Happi, G.M., Tsopgni, W.D.T., Waffo, A.F.K., Ndom, J.C., Wansi, J.D., 2021. Three new 30-norfriedelane and a new friedelane triterpenes from the trunk bark of *Caloncoba welwitschii* (Oliv.) Gilg (Achariaceae). Nat. Prod. Res.. https://doi.org/10.1080/14786419.2021.1981314.

Kim, K.H., Moon, E., Choi, S.U., Kim, S.Y., Lee, K.R., 2013. Polyphenols from the bark of *Rhus verniciflua* and their biological evaluation on antitumor and anti-inflammatory activities. Phytochemistry 92, 113–121.

Kweka, W.B.N., Talla, R.M., Jouda, J.-.B., Foudjo, M.G.L., Muhammad, S.A., Wandji, J., Mbazoa, C.D., 2022. Phytochemical analysis of the stems of *Angylocalyx oligophyllus* (Baker) f. (Fabaceae). Biochem. Syst. Ecol. 101, 104382.

Larayetan, R.A., Antimalarial, antitrypanosomal, antimicrobial activities and volatile oil profile of *Xylopia aethiopica* (Dunal) Rich (Annonaceae). Lett.Appl. NanoBioSci. 11, 3897–3908.

Lipinski, C.A., 2001. Avoiding investment in doomed drugs. J. Curr. Drug Discov. 1, 17–19.

Mbobda, A.S.W., Ngouonpe, A.W., Happi, G.M., Mountessou, B.Y.G., Monya, E., Jouda, J.B., Toussie, B.T., Lenta, B.N., Sewald, N., Kouam, S.F., Tchouankeu, J.C., 2021. Pachypodostyflavone, a new 3-methoxy flavone and other constituents with antifilarial activities from the stem bark of *Duguetia staudtii*. Planta Med. Int. Open 8, e56–e61.

Miranda, M.L.D., Garcez, F.R., Garcez, W.S., 2015. Triterpenes and other constituents from fruits of *Enterolobium contortisiliquum* (Vell.) Morong (Fabaceae). Rev. Virtual Quim. 7, 2597–2605.

Mutabingwa, T.K., 2005. Artemisinin-based combination therapies (ACTs): best hope for malaria treatment but inaccessible to the needy!. Acta trop 95, 305–315.

Ojewole, J.A., Adewunmi, C.O., 2004. Anti-inflammatory and hypoglycaemic effects of *Tetrapleura tetraptera* (Fabaceae) fruit aqueous extract in rats. J. Ethnopharmacol. 95, 177–182.

Phillips, M.A., White, K.L., Kokkonda, S., Deng, X., White, J., El Mazouni, F., Marsh, K., Tomchick, D.R., Manfalanagara, K., Rudra, K.R., Wirjanata, G., Noviyanti, R., Price, R.N., Marfurt, J., Shackleford, D.M., Chiu, F.C.K., Campbell, M., Jimenez-Diaz, M.B., Bazaga, S.F., Angulo-Barturen, I., Martinez, M.S., Lafuente-Monasterio, M., Kaminsky, W., Silue, K., Zeeman, A.-.M., Kocken, C., Leroy, D., Blasco, B., Rossignol, E., Rueckle, T., Matthews, D., Burrows, J.N., Waterson, D., Palmer, M.J., Rathod, P.K., Charman, S.A., 2016. A Triazolopyrimidine-Based Dihydroorotate Dehydrogenase Inhibitor with Improved Drug-like Properties for Treatment and Prevention of Malaria. ACS Infect. Dis. 2, 945–957.

Sahoo, R.K., Tamuli, K.J., Lhouvum, N., Dutta, D., Bordoloi, M., Sharma, H.K., Gogoi, K., Bhattacharyya, D.R., 2020. Phytochemical constituents from *Xanthium strumarium* L. and evaluation of their in vitro antimalarial activities. S. Afr. J. Bot. 135, 35–40.

Sanguinetti, M.C., Tristani-Firouzi, M., 2006. hERG potassium channels and cardiac arrhythmia. Nature 440, 463–469.

Seebacher, W., Simic, N., Weis, R., Saf, R., Kunert, O., 2003. Complete assignments of ^{1}H and ^{13}C NMR resonances of oleanolic acid, 18α-oleanolic acid, ursolic acid and their 11-oxo derivatives. Magn. Reson. Chem. 41, 636–638.

Sikam, K.G., Ntabo, V.K., Happi, G.M., Meikeu, L.Z., Wansi, J.D., 2022. Chemistry and pharmacological aspects of Aridanin, a lead compound from *Tetrapleura tetraptera* (Fabaceae). Natural Res. Hum. Health 3 (1), 1–6.

Song, N.-J., Yoon, H.-J., Kim, K.-H., Jang, W.-S., Seo, C.-R., Lee, Y.-M., Kweon, D-H., Hong, J.-W., Lee, J.-S., Park, K.-M., Lee, K.R., Park, K.W., 2013. Butein is a novel anti-adipogenic compound. J. Lipid Res. 54, 1385–1396.

Tabekoueng, G.B., Akak, C.M., Happi, G.M., Langat, M.K., Frese, M., Stammler, H.G., Neumann, B., Azebaze, A.G.B., Waffo, A.F.K., Wansi, J.D., Lenta, B.N., Sewald, N., Vardamides, J.C., Nkengfack, A.E., 2020. The chemistry of the West and Central African *Penianthus zenkeri* Diels (Menispermaceae). Phytochem. Lett. 38, 12–18.

Trager, W., Jensen, J.B., 1976. Human malaria parasites in continuous culture. Science 193, 673–675.

Trott, O., Olson, A.J., 2010. Software news and update AutoDockVina: improving the speed and accuracy of docking with a new scoring function, efficient optimization, and multithreading. J. Comput. Chem. 31, 455–461.

Tsaioun, K., Kates, S.A., 2010. ADMET For Medicinal chemists: a Practical Guide. John Wiley and Sons Ltd, Singapore.

Tsopgni, W.D.T., Happi, G.M., Stammler, H.-G., Neumann, B., Mbobda, A.S.W., Kouam, S.F., Frese, M., Azebaze, A.G.B., Lenta, B.N., Sewald, N., 2019. Chemical constituents from the bark of the Cameroonian mahogany *Trichilia emetica* Vahl (Meliaceae). Phytochem. Lett. 33, 49–54.

Wahab, O.A., Agana, T.A., Adu, F., Boakye, Y.D., Djameh, G.I., Boamah, D., 2021. Anti-trypanosomal and anthelminthic properties of ethanol and aqueous extracts of *Tetrapleura tetraptera* Taub. Vet. Parasitol. 294, 109449.

Williams, H.A., Durrheim, D., Shretta, R., 2004. The process of changing national malaria treatment policy: lessons from country-level studies. Health Policy Plan 19, 356–370.

Xiong, G., Wu, Z., Yi, J., Fu, L., Yang, Z., Hsieh, C., Yin, M., Zeng, X., Wu, C., Lu, A., Chen, X., Hou, T., Cao, D., 2021. ADMETlab 2.0: an integrated online platform for accurate and comprehensive predictions of ADMET properties. Nucleic Acids Res. 49, 5–14.

Yang, H., Lou, C., Sun, L., Li, J., Cai, Y., Wang, Z., Li, W., Liu, G., Tang, Y., 2018. admetSAR 2.0: web-service for the prediction of toxicity. Bioinformatics 35, 1067–1069.

View publication stats